

RESEARCH ARTICLE

A reliable electrochemical sensor developed based on ZnO/SnO₂ nanoparticles modified glassy carbon electrode

M. Mahmud Alam^{1*} M. T. Uddin¹ Mohammed M. Rahman^{2,3} Abdullah M. Asiri^{2,3} M. A. Islam¹¹ Department of Chemical Engineering and Polymer Science, Shahjalal University of Science and Technology, Sylhet 3100, Bangladesh² Chemistry Department, King Abdulaziz University, Faculty of Science, Jeddah 21589, Saudi Arabia³ Center of Excellence for Advanced Materials Research, King Abdulaziz University, Jeddah 21589, Saudi Arabia

Correspondence to: M. Mahmud Alam, Department of Chemical Engineering and Polymer Science, Shahjalal University of Science and Technology, Sylhet 3100, Bangladesh;
E-mail: alam-mahmud@hotmail.com

Received: March 26, 2021;**Accepted:** June 28, 2021;**Published:** July 1, 2021.

Citation: Alam MM, Uddin MT, Rahman MM, *et al.* A reliable electrochemical sensor developed based on ZnO/SnO₂ nanoparticles modified glassy carbon electrode. *Adv Biochips*, 2021, 2(1): 24-34.
<https://doi.org/10.25082/AB.2021.01.002>

Copyright: © 2021 M. Mahmud Alam, *et al.* This is an open access article distributed under the terms of the [Creative Commons Attribution License](https://creativecommons.org/licenses/by-nc/4.0/), which permits unrestricted use, distribution, and reproduction in any medium, provided the original author and source are credited.



Abstract: The 4-NPHyd (4-nitrophenylhydrazine) electrochemical sensor assembled using wet-chemically prepared ZnO/SnO₂ nanoparticle (NPs) decorated a glassy carbon electrode (GCE) with conductive Nafion binder. The synthesized NPs characterized by XPS, ESEM, EDS, and XRD analysis. The calibration of the proposed sensor obtained from current versus concentration of 4-NPHyd found linear over a concentration (0.1 nM ~ 0.01 mM) of 4-NPHyd, which denoted as the dynamic range (LDR) for detection of 4-NPHyd. The 4-NPHyd sensor sensitivity calculated using the LDR slope considering the active surface of GCE (0.0316 cm²), which is equal to be 7.6930 $\mu\text{A}\mu\text{M}/\text{cm}^2$, an appreciable value. The detection limit (LOD) at signal/noise (S/N = 3) estimated, and outstanding lower value at 94.63±4.73 pM perceived. The analytical parameters such as reproducibility, long-term performing ability and response time are found as appreciable. Finally, the projected sensor shows exceptional performances in the detection of 4-NPHyd in environmental samples.

Keywords: ZnO/SnO₂ nanoparticles, glassy carbon electrode, 4-Nitrophenylhydrazine sensor, sensitivity, environmental protection

1 Introduction

Generally, ZnO (zinc oxide) is a fascinating semi-conductor oxide (metal) to the material researcher for its promising physio-opto-electrochemical characteristics and terrifically it found to potentially apply in opt-electronic and electronic devices like light-emitting diodes [1], photo-detectors [2], photovoltaic cells [3], piezoelectric nano-generators [4], electroluminescence devices [5], gas sensor [6], chemical and biosensor [7, 8], nano-lasers [9] and flat display devices [10] and so on. Particularly, ZnO has a wider optical band gap of 3.3 eV and 60 meV binding for exciton [11, 12], the resistivity of $1 \times 10^{-3} \sim 1 \times 10^5$ W cm [13], stability [14] with optical transparency in the visible range. The conductivity of ZnO depends on intrinsic imperfectness like zinc interstitials and oxygen vacancies. The resistivity of ZnO for it,s wide bandgap energy can lower due to doping with the metal oxides of group III (B, Al, Ga, and In) and IV (Pb, Sn) in periodic-table [15, 16].

Several studies have shown that the nanocomposites of ZnO/SnO₂ have the better physio-electro-chemical properties compared to individual metal oxide in the application as Li-ion battery [17, 18], electrochemical sensors [19, 20] and catalyst [21, 22]. As the electrochemical sensing elements, the heterostructure of ZnO and SnO₂ can enhance the inner-electric fields within the nanoparticle interfaces. As a result, the electros transfer rate between the nanoparticles increase. Due to synergistic effects the ZnO and SnO₂ effects, the nanocomposites act like a buffer-matrix each to other for removing the stress and strain during electrochemical-reactions [23, 24]. Thus, this approach performed to develop an electrochemical sensor by wet-chemically prepared ZnO/SnO₂ NPs coated on GCE.

Due to the increasing the industrial activities, the water-soluble aromatic derivative of hydrazine coming from the untreated industrial effluent such as dyes, pesticides, photographic, plant-growth regulators, pharmaceuticals, colour and pigment industries. Besides this, the aromatic hydrazines use in explosive, rocket fuel and spacecraft fuel [25, 26]. The aromatic and aliphatic both hydrazine are poisonous for plants, animals, human and aquatic lives. Thus, hydrazine (aromatic and aliphatic) is known as carcinogenic, nephrotoxic, and environmental hazardous substance even at very lower concentration [27, 28]. The primary syndromes due to

exposure of hydrazine are respiratory oedema, Sight loss for short-term, vomiting-tendency, burning in eyes and nose. The long-term exposure of hydrazine might cause a serious effect on the liver and kidney, and it also affects the central nervous system, which leads to unconsciousness [29–31]. Therefore, a reliable technique for the detection of hydrazine (4-nitrophenylhydrazine) is necessary. In recent, many kinds of research have been conducted based on CoS₂-CNT nanocomposites [26], SrO.CNT NCs [27], Fe₂O₃ NPs [28], Co-doped ZSM-5 zeolites [25], TiO₂ nanoparticles [32], Fe₂O₃/CeO₂ nanocubes [33] and ZnO nanourchins [29] coated on GCE for precious hydrazines detection (both aromatic and aliphatic) applying electrochemical (I-V) approach.

This experimental work performed to assemble a sensor in I-V approach selective to 4-NPHy with ZnO/SnO₂ NPs coated on GCE. A calibration plot (current versus concentration of analyte) established satisfied by linearity regression co-efficient value ($R^2 = 99$). From the slope of the calibration curve, the sensor sensitivity measured. A signal/noise (S/N) ratio of 3 used to calculate the lower detection limit (LOD). In future, applying this technique to develop the electrochemical sensor using semi-conductive binary metal oxides on GCE will be prospective in the field of environment, on a large scale.

2 Experimental

2.1 Materials and methods

The analytical grade chemicals from Sigma-Andrich such as zinc acetate dihydrate, Zn(CH₃-COO)₂.2H₂O and tin tetrachloride (SnCl₄) were used to synthesize ZnO/SnO₂ NPs applying wet-chemical method in alkaline phase. The other necessary toxic chemicals known as hazardous to environment such as benzaldehyde, 4-aminophenol (4-AP), 4-nitrophenylhydrazine (4-NPHy), 2,4-diphenyldihydrochloride (2,4-DPDHCl), 3-chlorophenol(3-CP), 3-methoxyphenol (3-MP), M-tolyl hydrazine hydrochloride (M-THyHCl), zimaldehyde, 4-methoxyphenol (4-MP) and 3-methoxyphenylhydrazinehydrochloride (3-MPHyHCl) in analytical grade were also procured from the Sigma-Andrich USA. The auxiliary chemicals supporting to the study such mono- & disodium phosphate buffer and 5% nafion in ethanol were obtained from Sigma-Andrich also. The Thermo-Scientific XPS instrument containing Al-k- α 1 radiation sources with a beam of 300.0 μ m performed at 200.0 eV, and pressure 10-8 Torre was applied on the synthesized microstructures (nanomaterials) for the investigation of ionization states and binding energy of existing atoms. To confirm the structure and elemental compositions of synthesized metal oxides, the FESEM and EDS analysis were executed by an instrument model-JEOL, JSM-7600F (Japan). The grain size and crystalline plans of Ag₂O-doped ZnO NSs were assessed by the implementation of powder X-ray diffraction analysis. The electrochemical characterization of ZnO/SnO₂ NPs on GCE was examined through a Keithley electrometer as the source of constant supply of potential (volts).

2.2 Preparation method of ZnO/SnO₂ NPs

ZnO/SnO₂ NPs was prepared by homogenous precipitation method using Zn(CH₃COO)₂.2H₂O and SnCl₄ as precursors, and urea as a precipitating agent to form the alkaline phase. Following this typical method, 5.0 mL of SnCl₄ and 3.12 g (0.074 M) of Zn(CH₃COO)₂.2H₂O dissolved in 200 mL sized beaker and kept on a heater fixed at 90°C with the magnetic-stirring facility. Then, 30.0 g urea was added into the mixture and continued for 4 hours at these conditions. The co-precipitate of Zn(OH)₂.Sn(OH)₄.nH₂O obtain, and it assumed that the metal ions precipitated out totally at this high alkaline phase. Then, the resulted precipitates filtrated from the aqueous phase and successively washed with water (deionized) to remove alkalinity. Subsequently, the resultant mass placed inside an oven at 110°C overnight to execute the complete dry. Finally, the dry metal hydroxides mixture calcined at 500°C in a muffle furnace tentatively 6 hours at a flow of atmospheric air. At this elevated temperature, the metal hydroxides oxidize into oxides form as ZnO/SnO₂ nanomaterials. The obtained mixture of metal oxides then subjected to characterize by XRD, FESEM and XPS spectrometric analysis.

2.3 Modification of working electrode by ZnO/SnO₂ NPs

The central dominating part of the electrochemical sensor is working electrode. It assembled by a GCE coated with the synthesized ZnO/SnO₂ NPs. At the GCE modification process, ethanol used to form a slurry of ZnO/SnO₂ NPs and deposits on the flat part of GCE to obtain a thin layer of NPs. Then, the drying of it done by keeping at the laboratory ambient conditions.

For the long-time stability of deposited NPs layer on the GCE, the Nafion added. After that, the drying of modified GCE did by keeping into an oven at 35°C for an hour. A Keithley electrometer procured from Unite States (USA) used to connect ZnO/SnO₂ NPs/GCE and Pt-wire to perform as a working and counter electrodes. Then, 4-NPHyd solution at 0.1 mM diluted to several solutions varying concentrating in a range of 0.1n M ~ 0.1 mM to electrochemical (I-V) analyze. A calibration of the 4-NPHyd sensor using current versus concentration relation executed, and linearly confirmed by regression coefficient R². By identifying the concentration range fitted with R² = 0.99, the dynamic range (LDR) for 4-NPHyd detection denoted. The sensor sensitivity calculated applying the LDR slope over the active surface area of GCE (0.0316 cm²). The signal/noise ratio (S/N = 3) employed to find-out the low limit of detection (LOD) of 4-NPHyd. The mono- & disodium phosphate used as an equimolar concentration to prepare the buffer phase for electrochemical investigation. At electrochemical characterization of 4-NPHyd, the buffer phase in the investigation beaker taken 10.0 mL as constant throughout the study.

3 Results and discussion

3.1 Characterizations of ZnO/SnO₂ NPs by XPS analysis

The XPS analysis executed to evaluate the binding-energy and their oxidation number of atoms within the prepared ZnO/SnO₂ NPs in Figure 1. As the survey XPS spectrum perceived in Figure 1 (d), the obtained NPs contains only Zn2p, O1s and Sn3d orbitals. The Zn2p orbital is further sub-divided in the two asymmetric orbitals termed as Zn2p_{3/2} and Zn2p_{1/2} spin orbitals and located at 1022 and 1045 eV respectively with a separation of 23 eV, confirmed the Zn²⁺ ionization state in the NPs of ZnO/SnO₂ NPs demonstrated in Figure 1 (a) [34–37].

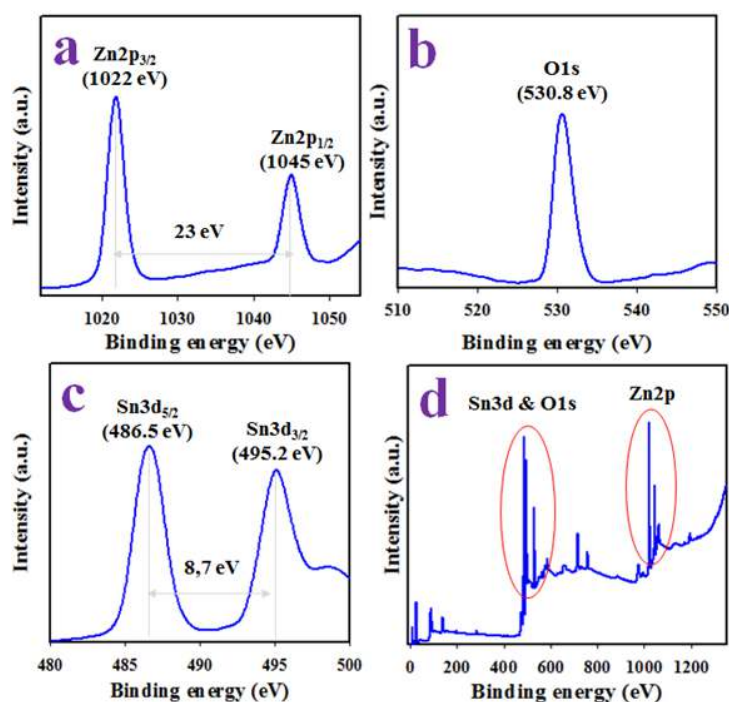


Figure 1 The XPS spectra of wet-chemically synthesized ZnO/SnO₂ NPs in alkaline phase. (a) The asymmetric spin orbitals of Zn2p level, (b) O1s peak, (c) the core level Sn3d orbited splitting into two spin orbitals of Sn3d_{5/2} and Sn3d_{3/2} and (d) the survey XPS spectra of ZnO/SnO₂ NPs.

The XPS spectral peak showing the high intensity located at 530.8 eV in Figure 1 (b) is identified of O1s and identified to lattice oxygen of ionization state of O₂⁻ in the prepared ZnO/SnO₂ NPs [38–40]. Besides this, the Sn3d level orbital in Figure 1 (c) is sub-divided in the two spin orbitals shown the binding energies of 486.5 and 495.25 eV related to Sn3d_{5/2} and Sn3d_{3/2} orbitals respectively. These spin orbitals separate with 8.7 eV a typical value confirms the Sn⁴⁺ oxidation identified by the earlier articles [41, 42].

3.2 The morphology of elemental compositions analysis of ZnO/SnO₂ NPs

The structural and atomic compositions of ZnO/SnO₂ nanomaterials identified by FESEM and EDS analysis.

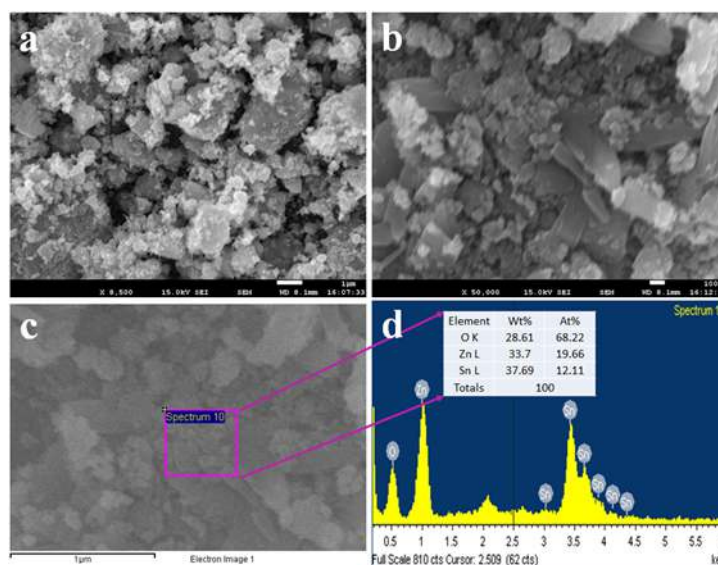


Figure 2 (a,b) The low and high magnifying images of ZnO/SnO₂NPs and (c,d) the EDS image and elemental analysis of NPs

A pictorial in [Figure 2 \(a\)](#) and [Figure 2 \(b\)](#), the magnifying (low and high) images of prepared nanomaterials, the ZnO, and SnO₂ nanomaterials are aggregated irregularly to form the nanoparticle shape with distinct sizes and shapes. The EDS image shown in [Figure 2 \(c\)](#) is conformed the same observation as in [Figure 1 \(a, b\)](#). The EDS elemental analysis illustrated in [Figure 2 \(d\)](#), the synthesized NPs contains 28.61% O, 33.7% Zn and 37.69% Sn only and the peaks associated with impurities are not detected.

3.3 The evaluation of phase crystallinity and particles size by XRD pattern

The XRD pattern of ZnO/SnO₂ NPs shows in [Figure 3](#), and X-ray powder diffraction (XRD) taken to identify the crystalline phases of ZnO-SnO₂ at the range of 20° ~ 80° with Cu K α 1 radiation ($\lambda = 1.5406 \text{ \AA}$). The reflected peaks regarding ZnO such as (002), (101), (110), (201), (004) and (202) plans can index following JCPDS (Joint Committee on Powder Diffraction Standards) card no 0089-1397 and previously reported articles of ZnO nanoparticles [43, 44]. Besides this, the identified peaks for SnO₂ such as (110), (211), (220), (311) and (301) plans are conformed by JCPDD No. 0036-1451 and previous authors [45, 46]. The average crystal size of synthesized NPs calculates applying the Scherer formula as $D = (0.94\lambda)/(\beta\text{Cos}\theta)$, and the estimated crystal size using ZnO(002) is 10.85 nm.

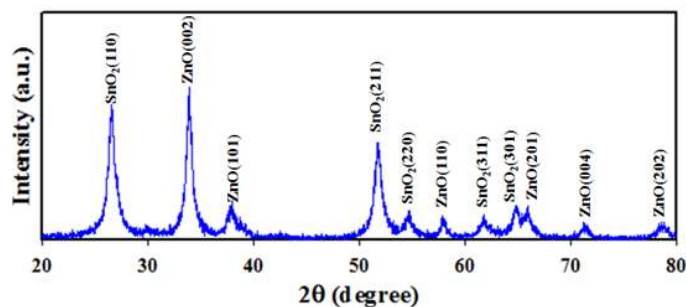


Figure 3 The XRD pattern of wet-chemically prepared ZnO/SnO₂ NPs

3.4 Sensor application of ZnO/SnO₂NPs/GCE Assembly

The selective 4-NPHyd sensor assembled by the coating of a GCE with ZnO/SnO₂ NPs as a layer of NPs and applied to the detection of 4-NPHyd at a buffer of pH 7.0. The long-time stability of NPs layer on GCE boosted by the addition of Nafion suspension. It should know that the Nafion used as a binder is a copolymer with conductive in nature. Thus, the use of Nafion on the modified GCE improves the conductance and the electron transfer rate of the resultant sensor. The similar characteristic of the sensor assembled using Nafion has reported in several articles to detect toxic chemicals [47–51]. The wet-chemically prepared ZnO/SnO₂ NPs on GCE as an electrochemical sensor to selective detection of 4-NPHyd is new and the information regarding its not available. During the electrochemical (I-V) sensing of 4-NPHyd in the buffer solution, the holding time in Keithley electrometer set 1.0 s as constant throughout the study. The amount of buffer solution for each I-V investigation took 10 mL in the measuring beaker.

The toxic chemicals in analytical grade such as benzaldehyde, 4-AP, 4-NPHyd, 2,4-DPDHCl, 3-CP, 3-MP, M-THydhCl, zimaldehyde, 4-MP and 3-MPHYdhCl were subjected to I-V investigation by assembled sensor based on ZnO/SnO₂ NPs/GCE at first illustrated in Figure 3 (a). The 4-NPHyd shows the supreme I-V outcome among the investigating toxics chemicals, which performed at 0.1 μ M and 0 ~ +1.5 V in 7.0 pH buffer phase presented in Figure 4 (a). Therefore, considering the highest I-V outcome, 4-NPHyd is categorised to selective toxic for the sensor assembly. Then, 4-NPHyd solutions in a range of 0.1 nM ~ 0.1 mM applied to analysis electrochemically at 0 ~ +1.5 V potential range in a buffer solution, and the resulted data represents in Figure 4 (b). The illustrated data in Figure 4 (b) exhibits a pattern to increase the I-V intensity with the increasing concentration of 4-NPHyd from lower to higher. This patter has described by previous authors in the detection of toxic chemicals in earlier [52–57]. The calibration of the 4-NPHyd sensor plotted in Figure 4 (c) known as a calibration curve. To execute this calibration, the current data separated from Figure 4 (b) at +1.5 volt. From the observation of Figure 4 (c), the current data are distributed linearly on the calibration curve from 0.1 nM to 0.01 mM of 4-NPHyd defined as the dynamic range of detection (LDR) and the linearity is satisfied by the regression co-efficient $R^2 = 0.9976$. The defined LDR has quite a wide range of detection of 4-NPHyd.

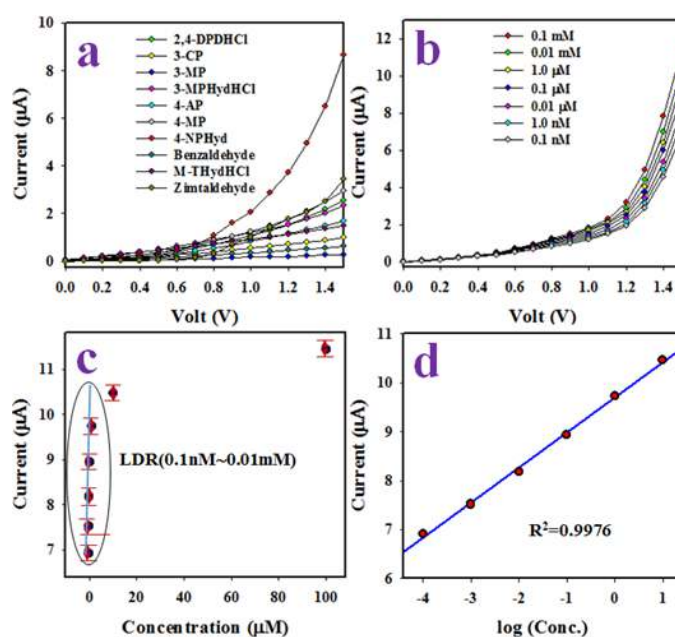


Figure 4 The electrochemical characterization of assembled sensor with ZnO/SnO₂ NPs/GCE. (a) the investigation of electrochemical responses of toxics chemical of 0.1 μ M in buffer phase, (b) I-V outcome of 4-NPHyd based on concentration, (c) the calibration of 4-NPHyd sensor and (d) current versus conc.

The sensor sensitivity using the calibration curve slope and active surface area of GCE (0.0316 cm²) is calculated and an appreciable sensitivity at 7.6930 μ A μ M/cm² perceive. The detection limit (LOD) of the 4-NPHyd sensor estimates by considering the signal/noise (S/N = 3) and the satisfactory LOD around 94.63 \pm 4.73 pM achieve.

The sensor response time expresses as a time to require the completion of an I-V analysis of

an analyte, and it is an efficiency measuring parameter. The response time of 4-NPHyd sensor tested at $0.1\mu\text{M}$ of 4-NPHyd in the buffer phase of pH 7.0 shown in Figure 5 (a). As perceived in Figure 5 (a), the current responses become steady around 22.0 s. Thus, the 4-NPHyd sensor needs 22.0 s to complete the I-V analysis of 4-NPHyd in the buffer phase. 22.0 s is quite enough to prove the high efficiency of the 4-NPHyd sensor with ZnO/SnO₂ NPs/GCE. The GCE was modified with SnO₂ NPs and ZnO/SnO₂ NPs to execute control experiments at $0.1\mu\text{M}$ 4-NPHyd and $0 \sim +1.5\text{ V}$ in a buffer solution as illustrated in Figure 5 (b). As in Figure 5 (b), ZnO/SnO₂ NPs/GCE electrode is exhibited the higher electrochemical activity compared to single SnO₂ NPs. It happens due to the combinational effects of both metal oxides. The reproducibility is reliability measuring parameter of the sensor and defines as the capability of the sensor to generate the unique I-V outcome in the identical conditions. The reproducibility test at $0.1\mu\text{M}$ of 4-NPHyd and $0 \sim +1.5\text{ V}$ in buffer phase of pH 7.0 was performed demonstrated in Figure 5 (c) in successive seven hours in a day. As shown in Figure 5 (c), the seven tests are unique and impossible to distinguish each to other. Thus, the 4-NPHyd sensor shows notable information that it is well enough to detect 4-NPHyd in unknown samples reliably. To measure the precision of reproducibility parameter in term of %RSD (relative standard deviation), the current data at $+1.5\text{ V}$ were subjected to check its precision and found 1.39% RSD, provides the high precision of reproducibility parameter. The stability of the sensor in the buffer phase is a very important criterion. To check this parameter of the 4-NPHyd sensor, the similar reproducibility tests but in successive seven days were executed illustrated in Figure 5 (d). The results alike reproducibility are perceived. This test conforms to the long-term stability of the sensor in the buffer phase with consistency in performance.

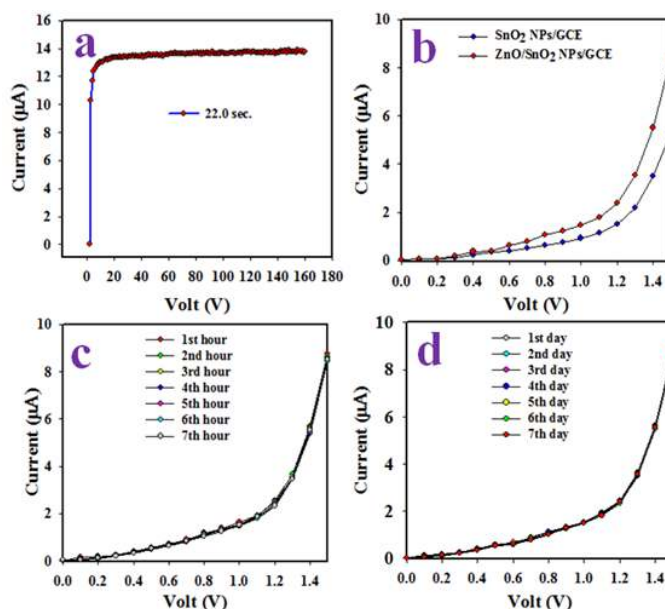


Figure 5 The tests of 4-NPHyd sensor based on ZnO/SnO₂ NPs/GCE to execute its reliability. (a) Response time, (b) the control experiments for 4-NPHyd sensor at $0.1\mu\text{M}$ 4-NPHyd and $0 \sim +1.5\text{ V}$ in buffer solution, (c) reproducibility test at $0.1\mu\text{M}$ 4-NPHyd and $0 \sim +1.5\text{ V}$ in buffer solution and (d) stability of 4-NPHyd sensor.

During the electrochemical detection of 4-nitrophenylhydrazine in buffer phase at applied potential, the 4-nitrophenylhydrazine molecules are adsorbed on the layered surface of ZnO/SnO₂ NPs and influence of potential, it is oxidized to 1,4-diaminobenzene and ammonium ion. Some-time, a number of free electrons are generated, which are responsible to enhance the conductance of sensing buffer medium and finally, I-V response is recorded in Keithely electrometer. Similar electrochemical oxidation has been mentioned in the earlier reports [58–60].

To execute the validation of this study, the researches of similar are compared with this study in-term of parameters such as sensitivity, LDR and detection limit (DL) as illustrated in Table 1 [61–63] and considering the parameters, the performances of this study is found as quite satisfactory and appreciable.

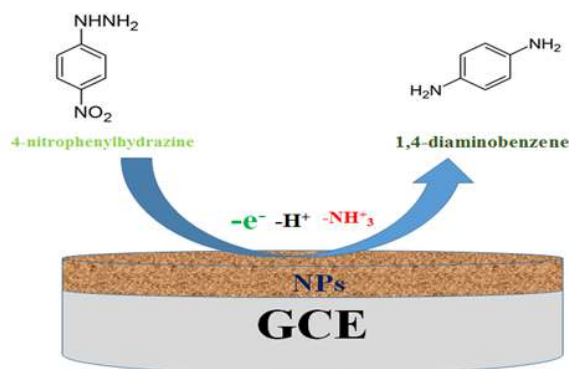


Figure 6 The electrochemical detection of 4-nitrophenylhydrazine in buffer phase with ZnO/SnO₂ NPs/GCE sensor probe.

Table 1 The comparison of analytical performances of 4-NPHyd sensors based on ZnO/SnO₂ NPs/GCE

Modified GCE	Analyte	*DL	#LDR	Sensitivity	Ref.
CoS ₂ /CNT NCs/GCE	Hyd	0.1 nM	0.1 nM ~ 1.0 mM	0.0044 $\mu\text{A}\mu\text{M}/\text{m}^2$	[61]
Sn/ZnO NPs/GCE	Hyd	18.9 pM	2.0 nM ~ 20.0 mM	5.0108 $\mu\text{A}\mu\text{M}/\text{m}^2$	[62]
T-PANI/Ag NCs/GCE	Hyd	2.8 nM	0.01 μM ~ 10 mM	12.5 $\mu\text{A}\mu\text{M}/\text{m}^2$	[63]
ZnO/SnO ₂ NPs/GCE	4-NPHyd	94.6 pM	0.1nM ~ 0.01mM	7.6930 $\mu\text{A}\mu\text{M}/\text{m}^2$	This work

Notes: *DL (detection limit), #LDR (linear dynamic range), pM(picomole), mM(millimole)

3.5 Analysis of real environmental samples

The validation of the proposed 4-NPHyd sensor based on ZnO/SnO₂ NPs/GCE in detecting 4-NPHyd was performed by applying recovery method. For this experiment, the samples known as real environmental samples collected as the extract of PC-water bottle, food packaging bag and sea and tape water. The analyzed data are presented in Table 2 and found as satisfactory.

Table 2 The analysis of real environmental samples using ZnO/SnO₂ NPs/GCE chemical sensor by recovery method

Sample	Added 4-NPHyd concentration (μM)	Measured 4-NPHyd conc. ^a by ZnO/SnO ₂ NPs/GCE(μM)			Average recovery ^b (%)	RSD ^c (%) (n = 3)
		R1	R2	R3		
Sea water	0.01	0.0104	0.0104	0.0106	104.54	1.1
PC- water bottle	0.01	0.0096	0.0094	0.0094	95.17	1.22
PVC- food packaging bag	0.01	0.0105	0.0106	0.0109	106.89	1.95
Tape water	0.01	0.0104	0.0103	0.0103	103.08	0.56

Notes: ^a Mean of three repeated determination (signal to noise ratio 3) ZnO/SnO₂ NPs/GCE; ^b Concentration of 4-NPHyd determined/Concentration taken. (Unit: nM); ^c Relative standard deviation value indicates precision among three repeated measurements(R1,R2,R3).

4 Conclusion

The wet-chemical prepared ZnO/SnO₂ NPs in alkaline phase were characterized by XPS, FESEM, EDS and X-ray diffraction at ambient condition. The prepared NPs were deposited on GCE to result 4-NPHyd sensor in buffer phase. A plot executed from concentration of 4-NPHyd versus current known as calibration curve and used to calculate sensor sensitivity, LDR and DL found as appreciable. The 4-NPHyd sensor parameters such as reproducibility, response time and long-time performing ability were tested and outstanding outcomes were exhibited.

Conflicts of interest

The authors declare that they have no known competing financial interests or personal relationships that could have appeared to influence the work reported in this paper. This manuscript has a preprint at Research square with DOI:10.21203/rs.3.rs-193392/v1

Acknowledgements

Center of Excellence for Advanced Materials Research (CEAMR), Chemistry Department, King Abdulaziz University, Jeddah, Saudi Arabia is highly acknowledged for financial supports and research facilities.

References

- [1] Na JH, Kitamura M, Arita M, *et al.* Hybrid junction light-emitting diodes based on sputtered ZnO and organic semiconductors. *Applied Physics Letters*, 2009, **95**(25): 253303-253305. <https://doi.org/10.1063/1.3275802>
- [2] Lu CY, Chang SJ, Chang SP, *et al.* Ultraviolet photodetectors with ZnO nanowires prepared on ZnO: Ga/glass templates. *Applied Physics Letters*, 2006, **89**(15): 153101-153103. <https://doi.org/10.1063/1.2360219>
- [3] Sudhagar P, Kumar RS, Jung JH, *et al.* Facile synthesis of highly branched jacks-like ZnO nanorods and their applications in dye-sensitized solar cells. *Materials Research Bulletin*, 2011, **46**(9): 1473-1479. <https://doi.org/10.1016/j.materresbull.2011.04.027>
- [4] Wang ZL, Yang R, Zhou J, *et al.* Lateral nanowire/nanobelt based nanogenerators, piezotronics and piezo-phototronics. *Materials Science and Engineering*, 2010, **70**(3-6): 320-329. <https://doi.org/10.1016/j.mser.2010.06.015>
- [5] Park WI and Yi GC. Electroluminescence in n-ZnO nanorod arrays vertically grown on p-GaN. *Advanced Materials*, 2004, **16**(1): 87-90. <https://doi.org/10.1002/adma.200305729>
- [6] Xu J, Han J, Zhang Y, *et al.* Studies on alcohol sensing mechanism of ZnO based gas sensors. *Sensors and Actuators B: Chemical*, 2008, **132**: 334-339. <https://doi.org/10.1016/j.snb.2008.01.062>
- [7] Uddin MT, Alam MM, Asiri AM, *et al.* Electrochemical detection of 2-nitrophenol using a heterostructure ZnO/RuO₂ nanoparticle modified glassy carbon electrode. *RSC Advances*, 2020, **10**(1): 122-132. <https://doi.org/10.1039/C9RA08669B>
- [8] Alam MM, Asiri AM, Uddin MT, *et al.* Detection of uric acid based on doped ZnO/Ag₂O/Co₃O₄ nanoparticle loaded glassy carbon electrode. *New Journal of Chemistry*, 2019, **43**(22): 8651-8659. <https://doi.org/10.1039/C9NJ01287G>
- [9] Huang MH, Mao S, Feick H, *et al.* Room-temperature ultraviolet nanowire nanolasers. *Science*, 2001, **292**(5523): 1897-1899. <https://doi.org/10.1126/science.1060367>
- [10] Park SB, Kim BG, Kim JY, *et al.* Field-emission properties of patterned ZnO nanowires on 2.5 D MEMS substrate. *Applied Physics A*, 2011, **102**: 169-172. <https://doi.org/10.1007/s00339-010-5981-9>
- [11] Ramadoss Ak and Kim SJ. Facile preparation and electrochemical characterization of graphene/ZnO nanocomposite for supercapacitor applications. *Materials Chemistry and Physics*, 2013, **140**(1): 405-411. <https://doi.org/10.1016/j.matchemphys.2013.03.057>
- [12] Benzarouk H, Drici A, Mekhnache M, *et al.* Effect of different dopant elements (Al, Mg and Ni) on microstructural, optical and electrochemical properties of ZnO thin films deposited by spray pyrolysis (SP). *Superlattices and Microstructures*, 2012, **52**(3): 594-604. <https://doi.org/10.1016/j.spmi.2012.06.007>
- [13] Ki Kim H, Sung Lee K and Ah Kang H. Characteristics of indium zinc oxide top cathode layers grown by box cathode sputtering for top-emitting organic light-emitting diodes. *Journal of Electrochemical Society*, 2006, **153**(2): H29-H33. <https://doi.org/10.1149/1.2139953>
- [14] Fang G, Li D and Yao BL. Fabrication and characterization of transparent conductive ZnO: Al thin films prepared by direct current magnetron sputtering with highly conductive ZnO(ZnAl₂O₄) ceramic target. *Journal of Crystal Growth*, 2003, **247**(3-4): 393-400. [https://doi.org/10.1016/S0022-0248\(02\)02012-2](https://doi.org/10.1016/S0022-0248(02)02012-2)
- [15] Bougrine A, El Hichou A, Addou M, *et al.* Structural, optical and cathodoluminescence characteristics of undoped and tin-doped ZnO thin films prepared by spray pyrolysis. *Materials Chemistry and Physics*, 2003, **80**(2): 438-445. [https://doi.org/10.1016/S0254-0584\(02\)00505-9](https://doi.org/10.1016/S0254-0584(02)00505-9)
- [16] Bian J, Li X, Chen L, *et al.* Properties of undoped n-type ZnO film and N-In codoped p-type ZnO film deposited by ultrasonic spray pyrolysis. *Chemical Physics Letters*, 2004, **393**(1-3): 256-259. <https://doi.org/10.1016/j.cplett.2004.06.044>
- [17] Belliard F and Irvine JTS. Electrochemical performance of ball-milled ZnO-SnO₂ systems as anodes in lithium-ion battery. *Journal of Power Sources*, 2001, **97-98**: 219-222. [https://doi.org/10.1016/S0378-7753\(01\)00544-4](https://doi.org/10.1016/S0378-7753(01)00544-4)
- [18] Ahmad M, Yingying S, Sun HY, *et al.* SnO₂/ZnO composite structure for the lithium-ion battery electrode. *Journal of Solid State Chemistry*, 2012, **196**: 326-331. <https://doi.org/10.1016/j.jssc.2012.06.032>

- [19] Yan SH, Ma SY, Xu XL, *et al.* Preparation of SnO₂-ZnO hetero-nanofibers and their application in acetone sensing performance. *Materials Letters*, 2015, **159**: 447-450.
<https://doi.org/10.1016/j.matlet.2015.07.051>
- [20] Yan SH, Ma SY, Li WQ, *et al.* Synthesis of SnO₂-ZnO heterostructured nanofibers for enhanced ethanol gas-sensing performance. *Sensors and Actuators B: Chemical*, 2015, **221**: 88-95.
<https://doi.org/10.1016/j.snb.2015.06.104>
- [21] Kong JJ, Rui ZB, Ji HB, *et al.* Facile synthesis of ZnO/SnO₂ hetero nanotubes with enhanced electrocatalytic property. *Catalysis Today - Journal*, 2015, **258**: 75-82.
<https://doi.org/10.1016/j.cattod.2015.04.011>
- [22] Lamba R, Umar A, Mehta SK, *et al.* ZnO doped SnO₂ nanoparticles heterojunction photo-catalyst for environmental remediation. *Journal of Alloys and Compounds*, 2015, **653**: 327-333.
<https://doi.org/10.1016/j.jallcom.2015.08.220>
- [23] Feng N, Qiao L, Hu DK, *et al.* Synthesis, characterization, and lithium-storage of ZnO-SnO₂ hierarchical architectures. *RSC Advances*, 2013, **3**(21): 7758-7764.
<https://doi.org/10.1039/c3ra40229k>
- [24] Luo L, Xu W, Xia Z, *et al.* Electrospun ZnO-SnO₂ composite nanofibers with enhanced electrochemical performance as lithium-ion anodes. *Ceramics International*, 2016, **42**(9): 10826-10832.
<https://doi.org/10.1016/j.ceramint.2016.03.211>
- [25] Rahman MM, Abu-Zied BM and Asiri AM. Ultrasensitive hydrazine sensor fabrication based on Co-doped ZSM-5 zeolites for environmental safety. *RSC Advances*, 2017, **7**(34): 21164-21174.
<https://doi.org/10.1039/C7RA00952F>
- [26] Rahman MM, Ahmed J, Asiri AM, *et al.* Development of highly-sensitive hydrazine sensor based on facile CoS₂-CNT nanocomposites. *RSC Advances*, 2016, **6**(93): 90470-90479.
<https://doi.org/10.1039/C6RA08772H>
- [27] Rahman MM, Hussain MM and Asiri AM. A novel approach towards hydrazine sensor development using SrO-CNT nanocomposites. *RSC Advances*, 2016, **6**(70): 65338-65348.
<https://doi.org/10.1039/C6RA11582A>
- [28] Akhter H, Murshed J, Rashed MA, *et al.* Fabrication of hydrazine sensor based on silica-coated Fe₂O₃ magnetic nanoparticles prepared by a rapid microwave irradiation method. *Journal of Alloys and Compounds*, 2017, **698**: 921-929.
<https://doi.org/10.1016/j.jallcom.2016.12.266>
- [29] Umar A, Akhtar MS, Al-Hajry A, *et al.* Enhanced photocatalytic degradation of harmful dye and phenyl hydrazine chemical sensing using ZnO nanourchins. *Chemical Engineering Journal*, 2015, **262**: 588-596.
<https://doi.org/10.1016/j.cej.2014.09.111>
- [30] Rahman MM, Khan SB, Jamal A, *et al.* Fabrication of Phenyl-Hydrazine Chemical Sensor Based on Al-doped ZnO Nanoparticles. *Sensors & Transducers Journal*, 2011, **134**: 32-44.
- [31] Nassef HM, Radi AE and O'Sullivan CK. Electrocatalytic oxidation of hydrazine at o-aminophenol grafted modified glassy carbon electrode: Reusable hydrazine amperometric sensor. *Journal of Electroanalytical Chemistry*, 2006, **592**(2): 139-146.
<https://doi.org/10.1016/j.jelechem.2006.05.007>
- [32] Rahman MM, Alfonso VG, Fabregat-Santiago F, *et al.* Hydrazine sensors development based on a glassy carbon electrode modified with a nanostructured TiO₂ films by electrochemical approach. *Microchimica Acta*, 2017, **184**: 2123-2129.
<https://doi.org/10.1007/s00604-017-2228-x>
- [33] Rahman MM, Alam MM and Asiri AM. Selective hydrazine sensor fabrication with facile low-dimensional Fe₂O₃/CeO₂ nanocubes. *New Journal of Chemistry*, 2018, **42**(12): 10263-10270.
<https://doi.org/10.1039/C8NJ01750F>
- [34] Rahman MM, Alam MM, Asiri AM, *et al.* Ethanol sensor development based on ternary-doped metal oxides (CdO/ZnO/Yb₂O₃) nanosheets for environmental safety. *RSC Advances*, 2017, **7**(37): 22627-22639.
<https://doi.org/10.1039/C7RA01852E>
- [35] Rahman MM, Alam MM, Asiri AM, *et al.* Fabrication of 4-aminophenol sensor based on hydrothermally prepared ZnO/Yb₂O₃ nanosheets. *New Journal of Chemistry*, 2017, **41**(17): 9159-9169.
<https://doi.org/10.1039/C7NJ01623A>
- [36] Alam MM, Asiri AM, Uddin MT, *et al.* Wet-chemically prepared low-dimensional ZnO/Al₂O₃/Cr₂O₃ nanoparticles for xanthine sensor development using an electrochemical method. *RSC Advances*, 2018, **8**(23): 12562-12572.
<https://doi.org/10.1039/C8RA01734D>
- [37] Rahman MM, Alam MM and Asiri AM. Carbon black co-adsorbed ZnO nanocomposites for selective benzaldehyde sensor development by electrochemical approach for environmental safety. *Journal of Industrial and Engineering Chemistry*, 2018, **65**: 300-308.
<https://doi.org/10.1016/j.jiec.2018.04.041>
- [38] Alam MM, Asiri AM, Uddin MT, *et al.* In-situ Glycine Sensor Development Based ZnO/Al₂O₃/Cr₂O₃ Nanoparticles. *ChemistrySelect*, 2018, **3**(41): 11460-11468.
<https://doi.org/10.1002/slct.201802750>
- [39] Alam MM, Asiri AM, Uddin MT, *et al.* One-step wet-chemical synthesis of ternary ZnO/CuO/Co₃O₄ nanoparticles for sensitive and selective melamine sensor development. *New Journal of Chemistry*, 2019, **43**(12): 4849-4858.
<https://doi.org/10.1039/C8NJ06361C>

- [40] Subhan MA, Jhuma SS, Saha PC, *et al.* Efficient selective 4-aminophenol sensing and antibacterial activity of ternary $\text{Ag}_2\text{O}_3\cdot\text{SnO}_2\cdot\text{Cr}_2\text{O}_3$ nanoparticles. *New Journal of Chemistry*, 2019, **43**(26): 10352-10365.
<https://doi.org/10.1039/C9NJ01760G>
- [41] Rahman MM, Alam MM and Asiri AM. Fabrication of an acetone sensor based on facile ternary $\text{MnO}_2/\text{Gd}_2\text{O}_3/\text{SnO}_2$ nanosheets for environmental safety. *New Journal of Chemistry*, 2017, **41**(18): 9938-9946.
<https://doi.org/10.1039/C7NJ01372H>
- [42] Rahman MM, Alam MM, Asiri AM, *et al.* Fabrication of selective chemical sensor with ternary $\text{ZnO}/\text{SnO}_2/\text{Yb}_2\text{O}_3$ nanoparticles. *Talanta*, 2017, **170**: 215-223.
<https://doi.org/10.1016/j.talanta.2017.04.017>
- [43] Saliyani M, Jalal R and Goharshadi EK. Effects of pH and Temperature on Antibacterial Activity of Zinc Oxide Nanofluid Against *Escherichia coli* O157: H7 and *Staphylococcus aureus*. *Jundishapur Journal of Microbiology*, 2015, **8**(2): e17115.
<https://doi.org/10.5812/jjm.17115>
- [44] Sagadevan S and odder JP. Investigation on Structural, Surface Morphological and Dielectric Properties of Zn-doped SnO_2 Nanoparticles. *Materials Research*, 2016, **19**(2): 420-425.
<https://doi.org/10.1590/1980-5373-MR-2015-0657>
- [45] Chen W, Zhou Q, Wan F, *et al.* Gas Sensing Properties and Mechanism of Nano- SnO_2 -Based Sensor for Hydrogen and Carbon Monoxide. *Journal of Nanomaterials*, 2012, 612420.
<https://doi.org/10.1155/2012/612420>
- [46] Janardhan E, Reddy MM, Reddy PV, *et al.* Synthesis of SnO Nanoparticles-A Hydrothermal Approach. *World Journal of Nano Science and Engineering*, 2018, **8**(2): 33-37.
<https://doi.org/10.4236/wjnse.2018.82002>
- [47] Rahman MM, Alam MM and Asiri AM. Potential application of mixed metal oxide nanoparticle-embedded glassy carbon electrode as a selective 1,4-dioxane chemical sensor probe by an electrochemical approach. *RSC Advances*, 2019, **9**(72): 42050-42061.
<https://doi.org/10.1039/C9RA09118A>
- [48] Rakib RH, Hasnat MA, Uddin MN, *et al.* Fabrication of a 3,4-Diaminotoluene Sensor Based on a $\text{TiO}_2\text{-Al}_2\text{O}_3$ Nanocomposite Synthesized by a Fast and Facile Microwave Irradiation Method. *ChemistrySelect*, 2019, **4**(43): 12592-12600.
<https://doi.org/10.1002/slct.201902394>
- [49] Rahman MM, Alam MM and Asiri AM. Detection of toxic choline based on $\text{Mn}_2\text{O}_3/\text{NiO}$ nanomaterials by an electrochemical method. *RSC Advances*, 2019, **9**(60): 35146-35157.
<https://doi.org/10.1039/C9RA07459G>
- [50] Rahman MM, Alam MM and Alamry KA. Sensitive and selective m-tolyl hydrazine chemical sensor development based on CdO nanomaterial decorated multi-walled carbon nanotubes. *Journal of Industrial and Engineering Chemistry*, 2019, **77**: 309-316.
<https://doi.org/10.1016/j.jiec.2019.04.053>
- [51] Abu-Zied BM, Alam MM, Asiri AM, *et al.* Fabrication of 1,2-dichlorobenzene sensor based on mesoporous MCM-41 material. *Colloids and Surfaces A*, 2019, **562**: 161-169.
<https://doi.org/10.1016/j.colsurfa.2018.11.024>
- [52] Rahman MM, Alam MM and Asiri AM. Development of an efficient phenolic sensor based on facile $\text{Ag}_2\text{O}/\text{Sb}_2\text{O}_3$ nanoparticles for environmental safety. *Nanoscale Advances*, 2019, **1**(2): 696-705.
<https://doi.org/10.1039/C8NA00034D>
- [53] Karim MR, Alam MM, Aijaz MO, *et al.* Fabrication of 1,4-dioxane sensor based on microwave assisted PAni-SiO₂ nanocomposites. *Talanta*, 2019, **193**: 64-69.
<https://doi.org/10.1016/j.talanta.2018.09.100>
- [54] Rahman MM, Wahid A, Alam MM, *et al.* Efficient 4-Nitrophenol sensor development based on facile $\text{Ag}@\text{Nd}_2\text{O}_3$ nanoparticles. *Materials Today Communications*, 2018, **16**: 307-313.
<https://doi.org/10.1016/j.mtcomm.2018.07.009>
- [55] Rahman MM, Alam MM and Asiri AM. Selective hydrazine sensor fabrication with facile low-dimensional $\text{Fe}_2\text{O}_3/\text{CeO}_2$ nanocubes. *New Journal of Chemistry*, 2018, **42**(12): 10263-10270.
<https://doi.org/10.1039/C8NJ01750F>
- [56] Rahman MM, Alam MM, Asiri AM, *et al.* 3,4-Diaminotoluene sensor development based on hydrothermally prepared MnCo_xO_y nanoparticles. *Talanta*, 2018, **176**: 17-25.
<https://doi.org/10.1016/j.talanta.2017.07.093>
- [57] Rahman MM, Alam MM and Asiri AM. Sensitive 1,2-dichlorobenzene chemi-sensor development based on solvothermally prepared FeO/CdO nanocubes for environmental safety. *Journal of Industrial and Engineering Chemistry*, 2018, **62**: 392-400.
<https://doi.org/10.1016/j.jiec.2018.01.019>
- [58] Sundaram S, Kumar AS, Jagannathan M, *et al.* In situ stabilization of hydroxylamine via electrochemical immobilization of 4-nitrophenol on GCE/MWCNT electrodes: NADH electrocatalysis at zero potential. *Analytical Methods*, 2014, **6**(22): 8894-8900.
<https://doi.org/10.1039/C4AY01994F>
- [59] Kaur B, Srivastava R and Satpati B. Copper nanoparticles decorated polyaniline-zeolite nanocomposite for the nanomolar simultaneous detection of hydrazine and phenylhydrazine. *Catalysis Science & Technology*, 2016, **6**(4): 1134-1145.
<https://doi.org/10.1039/C5CY01064K>

- [60] Hussain MM, Rahman MM and Asiri AM. Efficient 2-Nitrophenol Chemical Sensor Development Based on Ce₂O₃ Nanoparticles Decorated CNT Nanocomposites for Environmental Safety. PLOS ONE, 2016.
<https://doi.org/10.1371/journal.pone.0166265>
- [61] Rahman MM, Ahmed J, Asiri AM, *et al.* Development of highly-sensitive hydrazine sensor based on facile CoS₂-CNT nanocomposites. RSC Advances, 2016, **6**(93): 90470-90479.
<https://doi.org/10.1039/C6RA08772H>
- [62] Rahman MM, Balkhoyor HB and Asiri AM. Ultrasensitive and selective hydrazine sensor development based on Sn/ZnO nanoparticles. RSC Advances, 2016, **6**(35): 29342-29352.
<https://doi.org/10.1039/C6RA02352E>
- [63] Rahman MM, Khan A, Marwani HM, *et al.* Hydrazine sensor based on silver nanoparticle-decorated polyaniline tungstophosphate nanocomposite for use in environmental remediation. Microchimica Acta, 2016, **183**: 1787-1796.
<https://doi.org/10.1007/s00604-016-1809-4>